Biophysical Chemistry 27 (1987) 39–58
Elsevier

BPC 01131

Relation of growth process to spatial patterns of electric potential and enzyme activity in bean roots

Kiyoshi Toko [a], Satoru Iiyama [b], Chikako Tanaka [b], Kenshi Hayashi [a], Keiko Yamafuji [c] and Kaoru Yamafuji [a]

[a] Department of Electronics, Faculty of Engineering, Kyushu University 36, Fukuoka 812, [b] Department of Home Economics, Women's Junior College of Kinki University, Iizuka 820 and [c] Department of General Education, Faculty of Home Economics, Nakamura Gakuen College, Fukuoka 814, Japan

Received 21 January 1986
Revised manuscript received 12 December 1986
Accepted 14 January 1987

Electric potential; Acid elongation; Enzyme activity; Dissipative structure; Nonequilibrium; (Bean root)

The electric spatial pattern and invertase activity distribution in growing roots of azuki bean (*Phaseolus chrysanthos*) have been studied. The electric potential near the surface along the root showed a banding pattern with a spatial period of about 2 cm. It was found that the enzyme activity has a peak around 3–7 mm from the root tip, in good agreement with the position of the first peak of the electric potential, which is located a little behind the elongation zone. An inhomogeneous distribution of ATP content was also detected along the root. Experiments on the electric isolation of the elongation zone from the mature zone and acidification treatment showed that H^+ is transported from the mature-side to elongation-side regions, causing tip elongation through an acid-growth mechanism. Both acidification and electric disturbance on growing roots affected growth significantly. Simultaneous measurements of electric potential and enzyme activity clearly showed a good correlation between these two quantities and growth speed. From an analogy with the Characean banding, the spatio-temporal organization via the cell membrane in electric potential and enzyme activity can be regarded as a dissipative structure arising far from equilibrium. These experimental results can be interpreted with a new mechanism that the dissipative structure is formed spontaneously along the whole root, accompanied by energy metabolism, to make H^+ flow into the root tip.

1. Introduction

Spatial patterns of an electric potential and an electric current have often been observed in growth and regeneration processes. For example, a rhizoid formation in the brown alga *Fucus* is accompanied by an electric current pattern in the outside and inside of the egg [1]. Characean species develop alternating bands of acid and alkaline regions along their cell walls under illumination, and a localized elongation occurs in acid regions [2,3]; the electric potential near the cell surface also shows a similar pattern, with the electric current of H^+ flowing from the acid to the alkaline region [4].

Theoretical investigations [5–7] have shown that the band structure for Characean species is brought about by a simultaneous activation and inactivation of H^+ pump molecules within the plasmalemma along the cell, coupled with ADP (or ATP) and OH^- concentration gradients in the protoplasm. Such a band structure can be interpreted as a kind of self-organized structure appearing far from equilibrium through a nonlinear H^+ flux across the membrane, and hence belongs to dissipative structures defined by Gransdorff and

Correspondence address: K. Toko, Department of Electronics, Faculty of Engineering, Kyushu University 36, Fukuoka 812, Japan

Prigogine [8]. In the present case, the electric spatial pattern is maintained while the input energy supplied by light is dissipated continuously by both the active work of pump molecules inside the membrane and the viscous flow of H^+ in the media. The appearance of polarity succeeded by formation of an electric spatial pattern in *Fucus* algae can also be interpreted [7] as an occurrence of the dissipative structure; the self-organized state emerges through a positive feedback in nonlinear coupling between ion flux and accumulation of membrane-constituting molecules in the rhizoid region to grow.

The above theories have revealed that these electric spatial structures appearing in biological systems can be classified into the same kind of phenomena as the well-known 'chemical dissipative structures' in reaction-diffusion systems, represented by the Belouzov-Zhabotinskii reaction and Liesegang ring realizing far from equilibrium [8]. Such kinds of electric patterns observed in biological systems can then be named 'electric dissipative structures'. The experimental fact that these electric phenomena have been observed in many growing and regenerating cellular systems [9] strongly suggests a significant role of the electric dissipative structure in growth.

The purpose of the present paper is to study the relationship between the electric dissipative structure and growth in bean roots. A previous experimental work on a growing root of azuki bean [10] has clarified the following two points: (i) the root begins to display a band-type pattern of electric potential near the root surface with a spatial period of about 2 cm in a mature region, when it grows to 10 cm or so in root length; (ii) the growth speed is greatly diminished when the elongation zone is electrically isolated from the mature region. The band in the first item resembles quite well the banding phenomena in the Characeae, and the second may suggest a causal relation between the electric pattern and growth.

The fact that the acidification in the external aqueous medium did occur in the elongation zone under the usual conditions [10], as already reported [11], seems to be in strong support of the growth occurring through the wall expansion due to the acidification with the aid of acid growth mechanism [12]. At present, however, the relation between the conventional acid growth mechanism and electric pattern formation in growth has not been investigated very well, and hence is very obscure. This situation may be partly due to a lack of recognition that growth is a self-organization process with a dynamic interaction between biological systems and the environment through the electric field.

In the present paper, therefore, we investigate more detailed properties of the growth in respect of the electric spatial pattern from this viewpoint. Firstly, we measured the distributions of invertase activity, ATP and H^+-ATPase activity along the root. Secondly, the effect of tip acidification in roots under electric isolation was studied. Thirdly, we observed changes in invertase-activity distribution and electric pattern when roots were immersed in the acid solution. Fourthly the effect of an external electric disturbance on the growth was investigated. As a consequence, the invertase activity was found to have a characteristic peak around 5 mm behind the root tip in a similar manner to the electric potential. Inhomogeneous distributions of ATP and H^+-ATPase along the root were found. The acidification treatment induced an acceleration of initial growth, but later inhibited root elongation. In this case, the typical peak of enzyme activity gradually disappeared with time, parallel to the decrease in magnitude of the electrical potential along the root. Furthermore, the growth speed was extremely altered in the presence of an applied electric disturbance.

These experimental results clearly indicate an essential role of the global, active and dynamic properties of spatial electric-potential and enzyme-activity patterns along the entire root length, which emerge spontaneously in nonequilibrium conditions. We must, therefore, take into account these dynamic structures maintained under interactions with the electric circumstance in order to discuss the growth. In contrast, the acid growth mechanism proposed so far is limited only to a discussion of the elongation zone, i.e., a description of the local property. The new mechanism now suggested comprises the conventional acid growth mechanism even in a local sense. Furthermore, self-sustained oscillations of electric poten-

tial frequently observed in root growth [13–15] will be discussed in connection with a membrane-formation process in the elongation zone.

2. Materials and methods

The preparation of materials was as follows: seeds of azuki bean (*Phaseolus chrysanthos*) were soaked for 3 h, and then were sown on filter papers with 0.01 mM KCl solution in darkness at $30 \pm 1°C$. Roots emerged 1 or 2 days later. The 4–7-day-old roots were prepared for experiments using roots longer than 5 cm.

Luciferase-luciferin was obtained as firefly lantern extract (FLE-50) from Sigma. Pyruvic acid kinase, phospho*enol*pyruvic acid and amino-naphtholsulfonic acid were purchased from Sigma. Adenosine 5′-triphosphate disodium salt was the product of Boehringer Mannheim. Other chemicals used were of the finest grade available.

2.1. Measurements of electric potential and pH

The electric potential near the surface along a root was measured by each of the following two methods. The first is the usual method with a single-pipette electrode [4], which is filled with 1 mM KCl and 1% agar with a tip diameter of about 100 μm embedding an Ag/AgCl wire. A dark-grown root was laid horizontally on three filter papers in a plastic chamber and the 0.01 mM KCl aqueous solution was added to submerge the root. The potential close to the root surface was measured at each point of about 1-mm intervals by moving the electrode carefully by means of a manipulator. The electrode tip was located 0.5–1.0 mm from the root surface sufficiently carefully that direct contact with root was avoided. Within this range of distance from the root, the potential showed scarcely any dependence on distance. It took 30–40 min for one scan along a root of approx. 10 cm. The measurement was started at least 2 h after the root was placed in the chamber.

The method employed here differs from that above in using several ten-pipette electrodes. Fig. 1 shows the experimental setup of a multi-electrode system. Electrodes were arranged at 1.5-mm intervals along the root surface. The whole apparatus [16] is composed of these electrodes as sensors of electric potential, a hand-made circuit for sampling data adequately, a cassette recorder for storing the obtained data, and a personal computer for processing and arranging the data. We can finish one scan along the root within only 3 s with this apparatus. Although the careful arrangement of several tens of electrodes near the root surface is time-consuming work, this measuring method is superior to that relying on one electrode when considering the time required for actual measurement. Therefore, we mainly employed it for the investigation of temporal

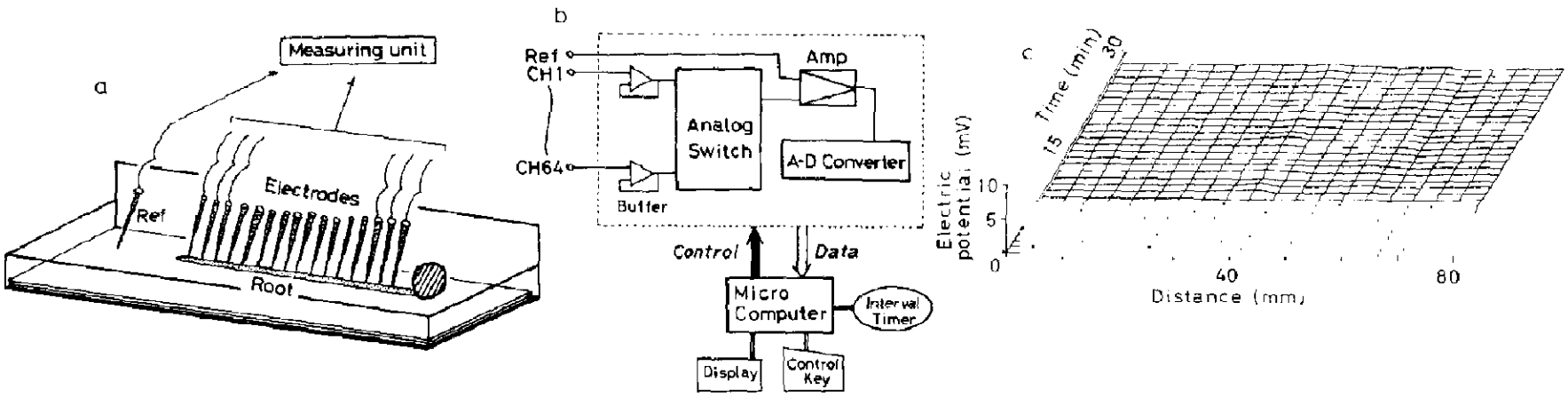

Fig. 1. Experimental setup (a) and measuring unit (b) of the multi-electrode apparatus with an example of measured electric potential in the aqueous medium (c). Pipette electrodes were arranged near the surface of the root with a reference electrode (Ref) separated from them. The root was usually laid on three filter papers moistened with 0.01 mM aqueous KCl. The maximum number of electrodes available for this apparatus is 64. In practice, 50 or 60 electrodes were sufficient for measuring the electric potential along the root for several centimeters. The time required for one scan over 64 electrodes is about 3 s. In (c), the stability of 20 electrodes was examined for 30 min in lining the electrode tips in the medium after the offset voltage was subtracted.

change in electric potential pattern along the root.

The offset voltage of one electrode used usually differed from another by approx. ±3 mV in the multi-electrode system. Here, the term offset denotes the sum of inherent electric voltages of individual pipette electrode and the electric circuit. Therefore, we subtracted the offset from the measured electric potential in the data processing. The offset in the aqueous medium was obtained after the measurement by removing the root gently. Fig. 1c shows the stability of 20 electrodes immersed in the medium after the offset was substracted at the start. A deviation of maximally ± 1 mV can be seen in the long run of 30 min. Thus, this kind of deviation appearing after several minutes causes no serious error in the evaluation of surface electric potential, because the offset was measured immediately after the actual measurement.

Observation of pH change along the root surface was made by placing a seedling in a medium containing 0.01 mM KCl and 0.2 mM bromocresol purple, adjusted to pH 6.8. For the more accurate measurement of pH values, a pH meter (Corning, model 125) equipped with a pH electrode (Iwaki Glass, model IW202) was used. The tip diameter of the electrode was smaller than 1 mm.

2.2. Measurements of ATP content and H^+-ATPase activity

A tip with 10 mm length of each bean root was cut into 10 small pieces. The resulting 1 mm pieces from the corresponding positions of five bean roots were combined and homogenized with a glass rod and extracted with 2.5 ml of boiling water for 8 min [17]. The extract was then filtered with a membrane and diluted with an equal volume of 0.08 M Tris-borate buffer (pH 9.2) for use in photometry performed according to a modified method of McElroy et al. [18]. 100 μl of the sample solution and 100 μl of 0.04 M Tris-borate buffer (pH 9.2) were placed in a microcuvette, to which 100 μl firefly lantern extract (10 mg in 1 ml of 0.05 M arsenate and 0.02 M $MgSO_4$) was added to start the reaction. The luminescence at 562 nm due to the formation of adenyloxyluciferin was measured with an Aminco Chem-Glow photometer. The intensity of light was integrated from zero to 100 ms. A standard curve was prepared with a solution of 100 ng ATP in 1 ml Tris-borate buffer (pH 9.2).

H^+-ATPase activity along the length of bean root from the tip was measured using five or ten roots in one assay. 1-mm pieces cut evenly from the roots were placed together in one test tube containing 0.82 ml ice-cold water and homogenized thoroughly with a glass rod. The amounts of phosphate produced by the hydrolysis of ATP by the root suspensions thus obtained were measured by the following procedure based on the method described by Kagawa [19]. To each suspension were added 0.1 ml of 50 mM ATP, $MgSO_4$ and phospho*enol*pyruvate in 200 mM Tris-sulfate buffer (pH 7.4) and 0.08 ml pyruvic acid kinase solution (400 μg/ml H_2O). After incubating the mixtures at 37°C for 10 or 30 min, the reaction was terminated by the addition of 0.5 ml of 20% tricholoroacetic acid. 0.5 ml supernatant solution was transferred into 3.25 ml water and mixed with 1 ml of 2.5% ammonium molybdate in 1 N sulfuric acid and 0.25 ml of 0.25% aminonaphtholsulfonic acid in 15% $NaHSO_3$ and 6% Na_2SO_3. After incubation at 30°C for 10 min, the absorbance at 660 nm was read using a Hitachi model 1010 spectrophotometer. Calibration was done with varying concentrations of potassium phosphate.

2.3. Measurements of enzyme activity

We studied the spatial distribution of acid invertase activity along the longitudinal axis of the root. One root was cut with 1-mm intervals from the root tip up to a length of 15 mm. Each segment was then put into each test tube separately. After 5 mM McIlvaine buffer solution (10 mM, pH 4.6) and 1 mM sucrose (10%) were added in the test tube, each segment was homogenized with a glass rod. Incubation was carried out at 37°C for 24 h, and then the invertase activity was measured according to Nelson [20] and Somogyi [21]. Thus, the activity pattern of invertase along one root was obtained.

When the effect of acidification or neutralization of the environment on root growth was

studied, ten individuals were used at the same time for measuring the invertase activity. This is due to the experimental result that the data obtained on one root are the same as the usual data averaged over several roots measured collectively, as will be detailed later. The time for the incubation was as short as 3 h when several individuals were collected and measured.

2.4. Electric isolation

The method of electric isolation of the elongation zone from the mature region is almost the same as those in previous works [10,22]. A special chamber with one thin wall of plastic plate is utilized for separating these two zones, as shown in fig. 2. A root was gently laid perpendicularly to the wall through an appropriate hole so that a few millimeters of the apical end and the basal part may be divided. Vaseline was applied around the root in the hole to isolate the two divisions electrically. Checking of the electric isolation was made by confirming that a very high electric resistance ($> 10^{10}$ Ω) existed between these two compartments.

The control is also shown in fig. 2. The partial mechanical shield was made merely in order to allow an electric connection between the two divided zones. The medium in each compartment was chosen as 0.01 mM KCl aqueous solution (pH 5.8), distilled water, acid buffer solution, etc., according to the experimental purpose. Growth was estimated by measuring the distance between the root tip and the point, which was indicated at a distance of 5 mm from the tip with Indian ink at the start of experiment. The electric potential in the presence of the plastic shield was measured with a single electrode by moving it along the root in the basal part.

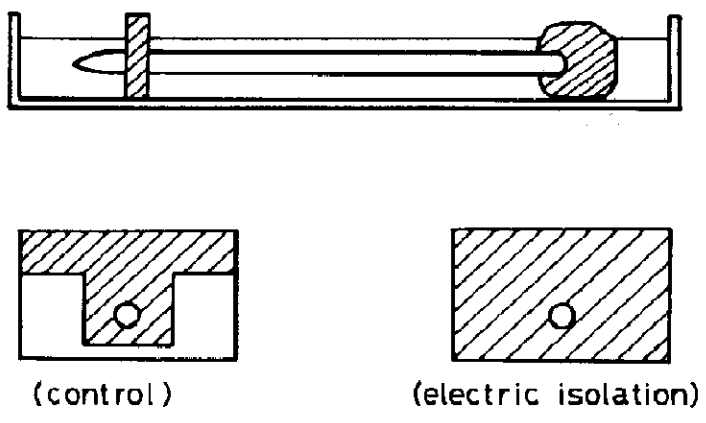

Fig. 2. Experimental setup for electric isolation of the elongation zone from the mature zone. The shield plate has a width of 2 mm with a hole. Vaseline was applied around the root part in the hole so that electric isolation could be made. The left part of the lower illustration concerns the control, where the shield was only partially made so as to allow electric connection between two compartments. The plate on the right has one hole alone for electric isolation.

2.5. Electric disturbance

To study the effect of an electric disturbance on the growth of bean roots, an electric conductor consisting of an aluminum plate coated with carbon black was inserted between two filter papers, on which a root was placed horizontally. Fig. 3a illustrates the cross-section of the experimental setup.

The electric conductor used here can be considered as a kind of electric cell. Many hollows of the density of four to five per cm^2 appeared rather randomly on the upper surface of plate. As shown in fig. 3b, the local electric current may flow from the naked aluminum part to the carbon black part. The apparently random electric disturbance can, therefore, be expected to add to the sponta-

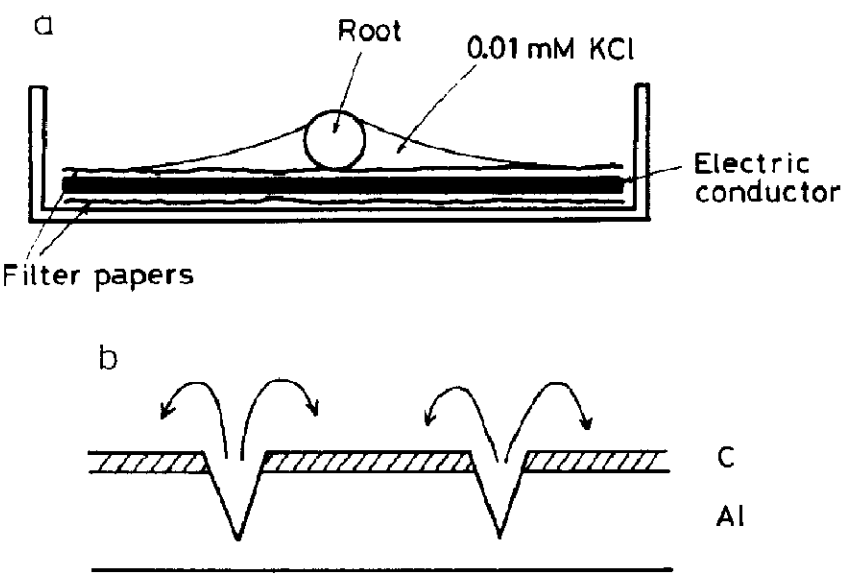

Fig. 3. Cross-section of the experimental setup (a) and an electric conductor coated with carbon black (b). The root was laid on two filter papers intercalated with the electric conductor. The carbon-coated Al plate behaves like an electric cell. The electric current arrow can flow around the hollow appearing rather randomly. It can disturb the original electric pattern in the root.

neous electric pattern produced by the root. The multi-electrode system was used to determine the resultant electric potential profile near the surface along the root.

Twenty roots of approx. 5 cm length were divided into two groups, control and test, and used for the growth experiment. In the control, roots were laid on two filter papers moistened with 0.01 mM KCl solution. The temperature was kept at $30 \pm 1°C$. Growth was estimated in the same way as for electric isolation.

3. Electric spatial pattern and acid elongation

3.1. Appearance of a spatial pattern of electric potential along a root

Fig. 4 demonstrates an example of data on electric potential near the surface along a root of 12.5 cm length. A periodic spatial pattern can be seen, analogous to the periodic appearance in Characean internodal or whorl cells [2,4]. In bean roots, however, the surface electric potential on the side of the root base is more positive than that near the root tip on the whole, as seen in fig. 4. Since the symmetry of the surface potential profile

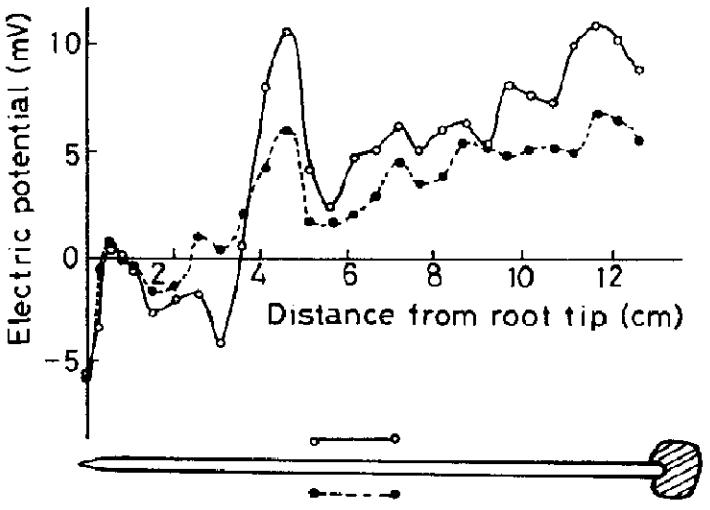

Fig. 4. Electric spatial pattern in a root. The units of the spatial coordinate are given in cm. The spatial change is rather periodic with about 2 cm period. The electric potentials on one side and the other side of a root surface are denoted by (○———○) and (●- - - - -●). The symmetry is fairly good, and hence this electric pattern can be supposed to exhibit a banding fashion. At the stage of 12 cm root length the epicotyl of about 5 cm elongates perpendicularly from the cotyledon; it is not drawn here.

on both circumferential sides of the root is fairly good, the electric potential can be considered as forming a band structure surrounding the root. This kind of pattern usually appeared when the root reached approx. 10 cm or so.

The band-type pattern of potential was stable in each root: a similar pattern was obtained when measurements were repeated within an interval as short as about 1 h. However, roots grew with an elongation velocity of about 1.5 mm/h, and hence in the long run the potential changed accompanied by the elongation, resulting in the production of another band. Thus, longer roots tended to exhibit more bands. When the root was as short as a few or several centimeters, on the other hand, the electric pattern tended to change occasionally (see the appendix).

The magnitude of a band is approx. 2 mV. While this value seems to be small, it is rather reproducible. The first experimental evidence is that almost the same periodic electric pattern within an accuracy of ± 0.3 mV can be obtained even after 1 h under good conditions such as when the root does not add a new peak with the elongation, as mentioned above. The second is that we can observe the same pattern even if the arrangement of electrodes is changed arbitrarily in the case of the multi-electrode system. Thirdly, the circumferential symmetry is fairly good (see fig. 4), i.e., there is only a small possibility of experimental errors casually producing such symmetry. Finally, there is the good stability of electrodes as can be seen from fig. 1c, where an abrupt change of ± 2 mV in the potential does not occur. This conclusion is similar to the case of electric measurement made in Characean banding [4]. In this system a banding change of 4–8 mV is also observed using the pipette electrode.

Fig. 5 shows examples of surface potential and growth speed near the root apex. The elongation zone is mostly located 1–3 mm behind the tip, in accord with previous reports [23,24]. The surface electric potential, on the other hand, has a positive peak at 5–8 mm behind the tip, while the flat part exists at 2–3 mm. This means that the potential is relatively negative in the elongation zone. This may suggest the existence of electric influx in this zone as a whole.

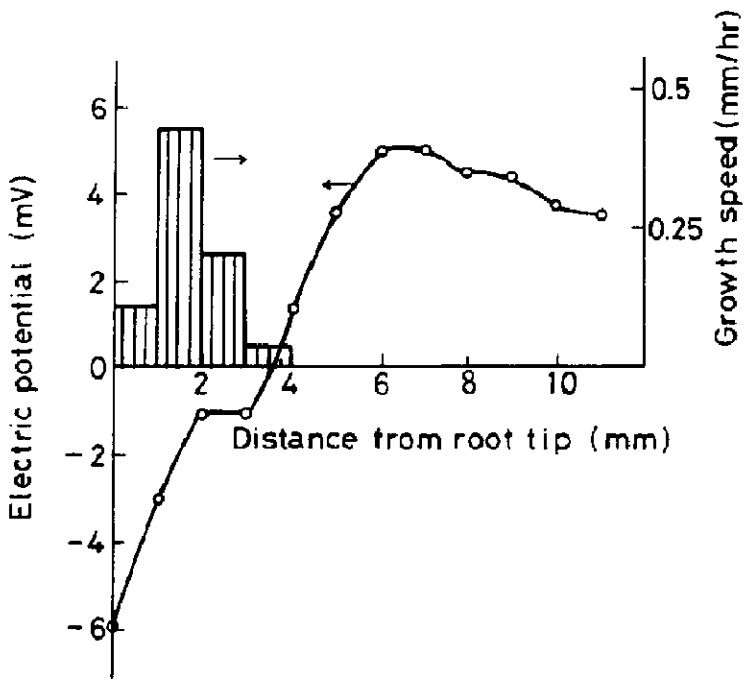

Fig. 5. Electric potential and growth speed at each point of the root near the tip at 30±1°C. Note that the units of length are expressed as mm. The elongation zone is located 2–3 mm from the tip and a peak of electric potential lies around 5–8 mm, i.e., in the mature zone. The length of root used for the potential measurement is 9 cm. Whereas the root is different from that in fig. 4, a large peak can be seen at almost the same position around 6 mm.

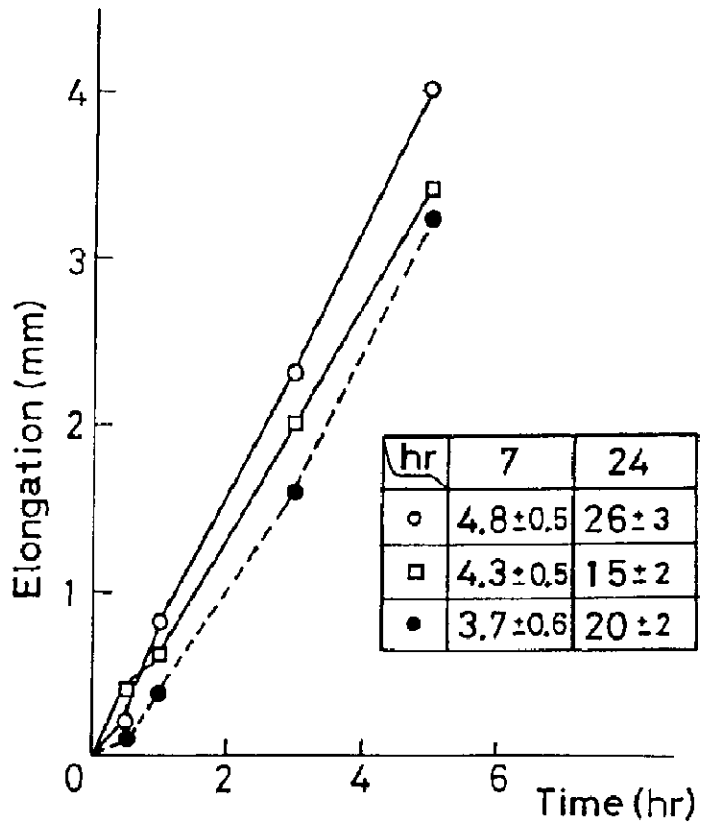

Fig. 6. Result of electric isolation and effect of acidification. (○——○) Control, (□——□) electric isolation plus HCl treatment and (●- - - - -●) electric isolation at 25±1°C with 30 roots for each group. Inset: table for elongation after 7 and 24 h. The values given are the means±deviation. The roots under electric isolation always showed a slower growth speed than the controls. The roots under electric isolation plus acidification treatment grew more rapidly than the control initially, but later grew at the slowest speed.

3.2. *Electric current and acid elongation*

A participant role of electric events in growth can be demonstrated by electric isolation of the elongation zone from the mature zone. Fig. 6 shows that electric isolation does suppress the growth. The roots under electric isolation had a growth speed a few ten percent lower than that of the control roots. Ten roots were placed on filter papers moistened with distilled water for each kind of experiment, which was repeated three times. The average values of results are adopted in fig. 6. The reason why the elongation is relatively small at the initial stages of 30 min in the control group is that the rear part of the elongation zone and the front part of the mature zone are shielded by a plastic plate, which may diminish the electric current around the root even if a large space is made on both sides of the plate (see fig. 2). Complete cessation of growth did not occur partly because consummate isolation could not be made: the root surface always became moist even if the moisture was wiped off with filter papers.

The results in fig. 6 can be interpreted as being caused by the interruption of fluent ionic flow into the elongation zone from the mature region. Table 1 lists values of the pH near the root in elongation and mature zones in external bulk solution pH of 6.65. Twenty roots were used for each experiment. The result shows that a decrease in pH in the elongation zone occurs in the control group, whereas it scarcely occurs when the elonga-

Table 1

pH in the elongation-zone and mature-zone compartments under electric isolation

Measurements were made with a pH meter equipped with a pH electrode. The pH in the external medium was set to 6.65±0.15. The pH values at about 1 and 5 mm from the root tip were measured after 10 min from the start of the experiment.

	Elongation zone	Mature zone
Electric isolation	6.58±0.25	5.92±0.10
Control	6.18±0.08	6.29±0.07

tion zone is electrically isolated: this zone became more acidic than the mature region under normal conditions. On the other hand, the mature region became more acidic under electric isolation. Taking into account that the surface electric potential in the mature region is relatively positive, we can consider that H^+ flows from the mature region through the external medium into the elongation zone. Thus, H^+ accumulates in this zone. This leads to wall expansion through the acid growth mechanism.

If this conclusion is valid, the growth speed is expected to recover somewhat when we intentionally add H^+ in the elongation zone even under electric isolation. 5 ml HCl solution (pH 4.0) was added to the compartment containing the elongation zone, and distilled water was poured into another compartment containing the mature region. Treatment at pH 4 is frequently made for investigation of acid growth [24]. This result is also illustrated in fig. 6. As expected, the growth speed in this treatment was distinctly greater than that under electric isolation only. Rather surprisingly, elongation at early stages during 30 min was evident compared with the control. This noticeable growth is due to facilitated wall expansion brought about intentionally by the extreme acidification, even if the supply of H^+ from the backward region of root is interrupted under electric isolation.

After 24 h had elapsed, however, roots under electric isolation plus HCl treatment did not grow as extensively as groups under electric isolation. As already mentioned, roots could grow partly because of incomplete isolation. Roots under electric isolation could grow at the normal velocity, as soon as the mature region was formed in the front compartment where the elongation zone had existed at the start of the experiment. This is because the electric isolation no longer exists between the elongation zone and the newly formed mature zone. In groups under electric isolation plus HCl treatment, on the other hand, the newly formed mature region in the front compartment is always exposed to the imposed low pH. This implies the destruction of the spatial pattern of H^+ produced by the root itself. The retardation of growth can be considered as being due to the impossible construction of an H^+ concentration pattern along the root adequate for growth. This point will be examined in later sections.

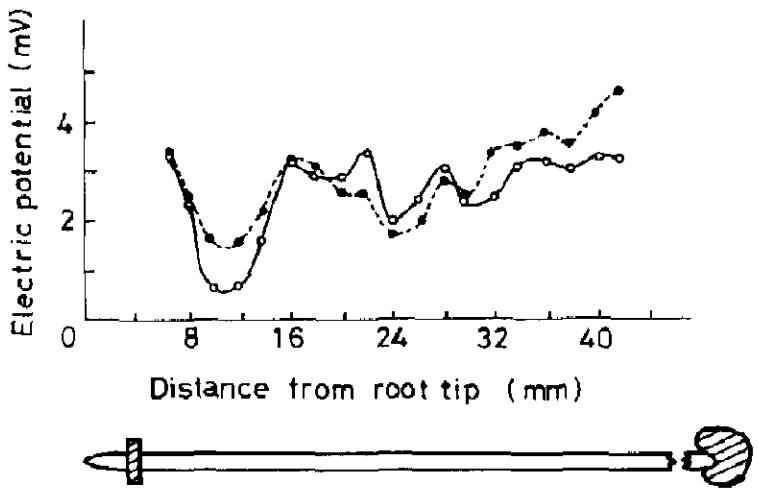

Fig. 7. Potential profile in roots of about 5 cm length with (●- - - - -●) and without (○———○) electric isolation. The units of the spatial coordinate are in mm. The two are almost the same in the mature zone. The electric potential in the elongation zone could not be measured due to the very short length of a few millimeters.

Fig. 7 shows that the electric potential profile scarcely changed even when electric isolation was performed. The data on the mature-region side are shown. Reliable measurement of the pattern in the elongation-region side could not be made because this side is very narrow, viz. a few millimeters. The result in fig. 7 may imply that the electric current flowing to the elongation zone is a direct factor for the growth rather than the electric potential. In general, the electric current of H^+ may be produced by the H^+-ATPase at the root surface, and the electric potential may reflect the pump action, as demonstrated by strong hyperpolarization under illumination in the Characeae [25,26]. The above result may therefore suggest that the pump action along the root is scarcely altered by the electric isolation. This agrees with the interpretation in table 1 that the tip acidification was directly suppressed, to retard the growth through interruption of the electric current.

3.3. Accumulation of H^+ and electric potential difference

From the above argument, H^+ can be considered to flow in the external medium from the mature-region side to the elongation zone, where

H^+ accumulates to cause the wall expansion. We shall now examine the relation of H^+ accumulation to the electric potential difference existing between the elongation and mature zones (see fig. 5). While an electric current flows along the root, this value is as small as several $\mu A/cm^2$ in barley roots [27]. In contrast, a large electric current of several tens of $\mu A/cm^2$ is reported for Characean cells [28] and a few mA/cm^2 flows in the nerve excitation [29].

Therefore, we can also expect such a small current in roots of azuki bean as observed in barley roots. In this case, the H^+ accumulation can be regarded as occurring in a situation close to equilibrium. It will permit one to consider the electrochemical potential in the aqueous phase near the surface in the elongation zone as being equal to that in the mature zone. Let μ denote the electrochemical potential, then the above statement reads

$$\mu_e = \mu_m, \tag{1}$$

where the subscripts e and m imply the elongation and mature zones, respectively. The explicit equation leads to

$$\mu_0 + k_B T \log[H^+]_e + e\psi_e = \mu_0 + k_B T \log[H^+]_m + e\psi_m, \tag{2}$$

where μ_0 designates the standard chemical potential, k_B Boltzmann's constant, T the absolute temperature, e the positive elementary charge, $[H^+]$ the proton concentration and ψ the electric potential near the root surface.

Rewriting eq. 2, we obtain

$$0.0166(\psi_m - \psi_e) = pH_m - pH_e, \tag{3}$$

where the definition of pH was used and the numerical coefficient was estimated at $T = 30\,^\circ C$ in units of pH/mV. From this equation, we expect that the pH difference amounts to approx. 0.12 by using the potential difference of 7.5 mV typically estimated from fig. 5. This value agrees fairly well with that observed, for example, $pH_m - pH_e = 0.11$ given in table 1. Thus, diffusion of H^+ from the elongation to mature zones caused by the concentration gradient may somewhat balance the flow from the mature to elongation zones originating in the electric potential difference.

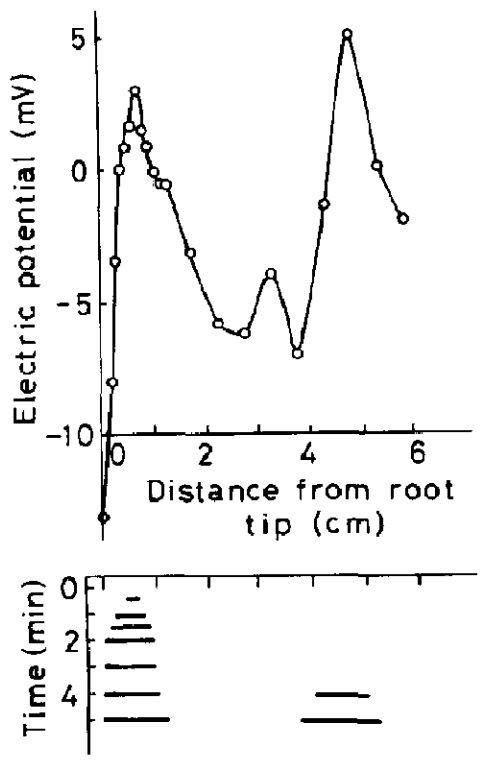

Fig. 8. Time course of pH extending along the root surface (units: cm). The time refers to the passage from cessation of the agitation of the external aqueous medium. The root length is 6 cm. The thick bars show the regions which became yellow in the presence of bromocresol purple. Two distinct acidified regions can be seen, each of which originates in the peak of the surface electric potential at each position.

The time course of the pH extending along the root surface is shown in fig. 8. Soon after agitation of the external aqueous medium containing 0.2 mM bromocresol purple, a position around 6 mm behind the root tip became yellow. The region comprising the semi-matured elongation zone and the young mature region became acidic first. This initial acidic change can be acknowledged, because the peak of the surface electric potential is located quite near this region, i.e., around 7 mm behind the tip. The acidified region, however, extended gradually to both directions of the tip and base sides. The resultant pH profile may be formed according to the above equilibrium condition of the electrochemical potential. Two spatially separated acidified regions were formed 5 min later. Each originates in each potential peak formed along the root surface.

4. Enzyme activity, ATP and H^+-ATPase distributions along roots

Fig. 9 shows two results on the invertase activity distribution along a root measured according

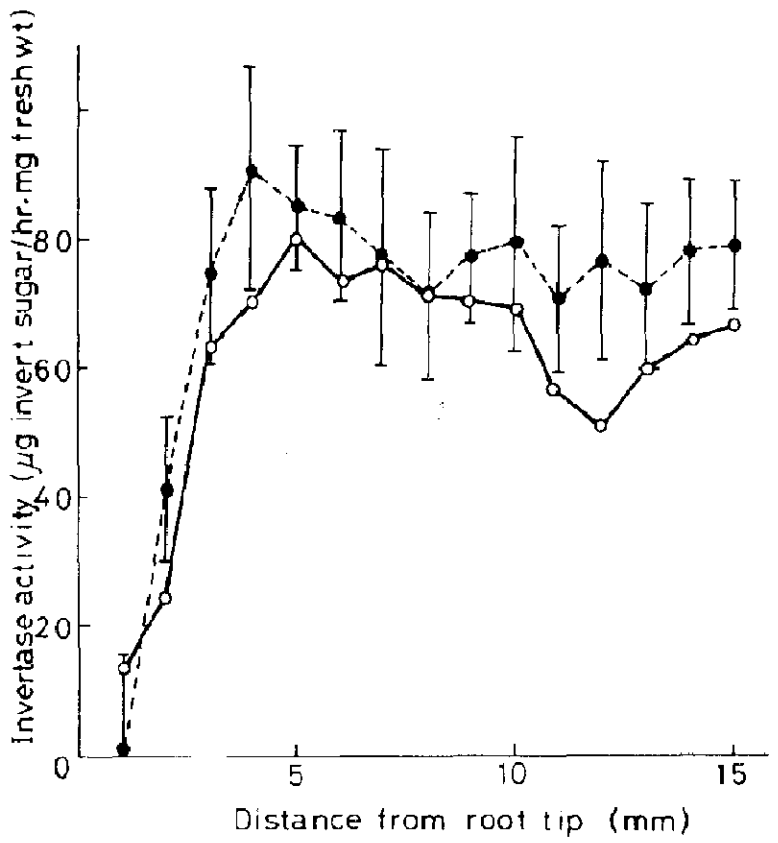

Fig. 9. Invertase activity along a root. The result measured in one root (○——○) is compared to that averaged over data on ten roots measured collectively as usual (●- - - - -●), with the vertical bar denoting the variance. The collected measurements were made 6 times for sets of 10 roots of length 3–10 cm. The agreement between them is good, showing a peak around 3–7 mm behind the tip.

to two different methods. One result was obtained by measuring the invertase activity in one root. Each root used independently showed almost the same spatial distribution of invertase activity. Another result was obtained by collecting segments from ten roots at the same time in each test tube and then measuring the invertase activity, as is usually done [30–32].

We can see that both results agree well. This indicates reliability of measurement of enzyme activity using one root, which has not been performed yet. The invertase-activity distribution in fig. 9 exhibits a typical pattern with a peak around 3–7 mm from the root tip. If we compare this pattern with those of growth speed and electric potential shown in fig. 5, we observe that the activity distribution resembles the electric potential pattern.

The good correlation between invertase activity and electric potential can be interpreted as follows: the high electric potential near the root surface may partly reflect the active work of H^+ pumps within the cell membrane at the surface. In such a region, energy production as well as consumption occurs rather vigorously. Thus, this leads to high activity of invertase, which is an enzyme dissolving sucrose as an energy source in beans [33].

Although the relation of invertase activity to the elongation zone has been discussed [31], its relation to the electric potential has not been demonstrated. This may be due to the lack of detailed measurements of both the position of the elongation zone and the electric potential. A comparison of data on the position of the elongation zone in fig. 5 with those on the electric potential (fig. 5) and enzyme activity (fig. 9) reveals that the position of the elongation zone (2–3 mm) differs from the peak positions (approx. 3–8 mm) of the latter two. The most active position of H^+ pumps within the cell membrane may be a little behind the elongation zone. Since a small peak or flat part can often be seen around 2–3 mm as shown in figs. 5 and 12, however, the semi-matured elongation zone can also be considered to become an H^+ source in cooperation with the mature region. It appears that H^+ is extruded through the membrane in the mature region and the semi-matured elongation zone. This inference based on the enzyme activity distribution agrees with the interpretation made in section 3 that H^+ accumulating in the elongation zone originates from the mature region behind it.

Fig. 10 shows the ATP content in each 1 mm root segment near the root tip. The ATP content begins to drop at the segment 5–6 mm from the tip. This tendency seems to coincide with the peaks of electric potential and invertase activity. Thus, it might be interpreted as follows: this region acts as an H^+ source for the external medium, which inevitably leads to the consumption of ATP. However, this cannot be asserted since the H^+ transport concerned now refers to the root surface, and the ATP content in fig. 10 also refers to the inside of root.

The dependence of the rate of ATP hydrolysis on the amount of root used in one incubation and the effect of the incubation time are shown in fig. 11a. Here, H^+-ATPase activity is plotted as nmol

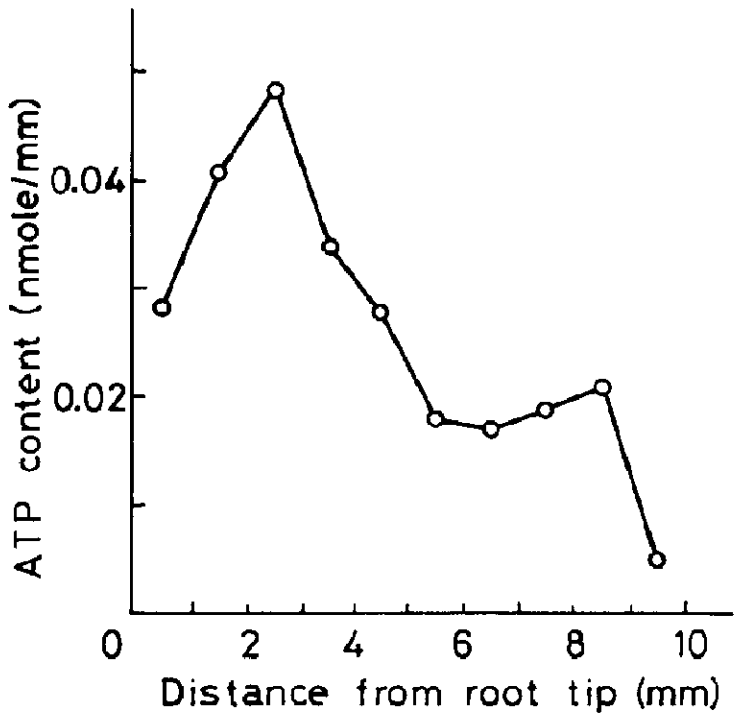

Fig. 10. ATP content in each 1 mm root segment near the root tip. The length of roots used is about 5 cm.

phosphate released in the total (1 ml) incubation mixture, namely, nmol ATP hydrolyzed by total root segments (5 or 10 1-mm pieces) used in one incubation mixture.

By converting these data to the specific rate of hydrolysis (nmol ATP hydrolyzed by one 1-mm segment in 1 min), we obtain the plot of the mean value, as shown in fig. 11b. This shows that H^+-ATPase is concentrated 1–2 mm from the tip and rather diluted at the very tip or 6–7 mm from the tip. The interpretation of these data seems to need careful consideration. The measured H^+-ATPase activity is concerned with the parenchyma as well as the organ surface. The relationship, therefore, between the obtained result of H^+-ATPase activity and the membrane transport partly reflected by the surface electric potential is obscure at the present stage. Nevertheless, such an inhomogeneous distribution is suggestive of its electrochemical and biophysical importance in growth.

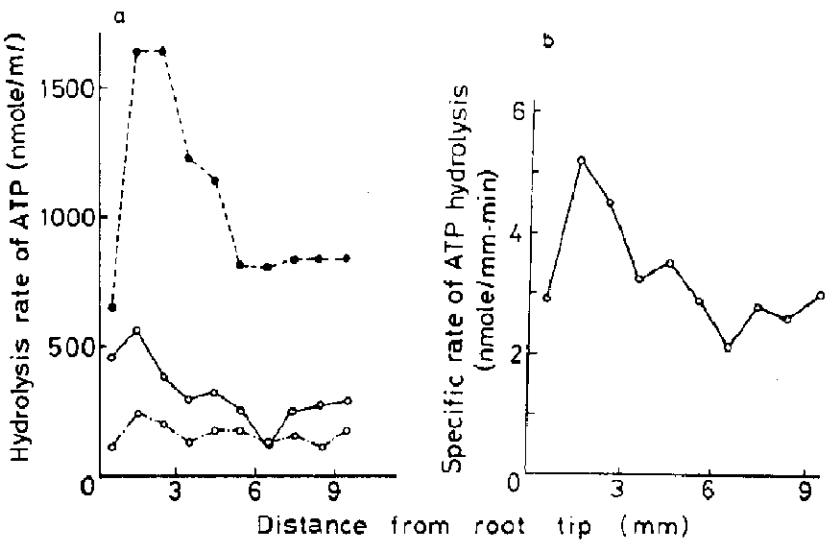

Fig. 11. Hydrolysis rate of ATP (a) and specific rate of ATP hydrolysis (b). The root length is about 5 cm. In (a), the curve (○———○) shows the incubation time 10 min for 10 collected roots (○- - -○) 10 min for 5 roots, and (●- - - - -●) 30 min for 10 roots. These curves are from three separate specimens.

5. Entire acidification of root

The result in fig. 6 can be interpreted as follows: the root can grow rather fast because of the facilitated acid elongation at the early stages. However, the further elongation at later stages is suppressed owing to entire acidification along the elongation and mature zones of root, which results in the disappearance of the H^+ concentration pattern adequate for growth. If this conjecture is correct, the root immersed in acidic solution may be expected to experience a similar time course. Whereas measurements of the electric potential and invertase activity along the root under electric isolation could not be made very easily because of the mechanical fixation of the root to the bottom of the experimental vessel (see fig. 2), we could perform them for the present case. Thus we investigated more closely the effect of acidification on growth from two kinds of measurements of electric potential and invertase activity.

5.1. Growth in acidic medium

Fig. 12 gives the results of acidification treatment of roots. Thirty roots were divided into three groups in distilled water, 2 mM acetate buffer (pH 4.0) and HCl solution (pH 4.0). The 2 mM acetate buffer has been frequently used in experiments using a root segment concerning the acid growth mechanism [34,35].

In carrying out the above experiment, we inclined the vessel at an angle of approx. 10° so that the root could be immersed in the medium sufficiently, as illustrated in fig. 13a. If we retained the vessel horizontally as is usual, the roots

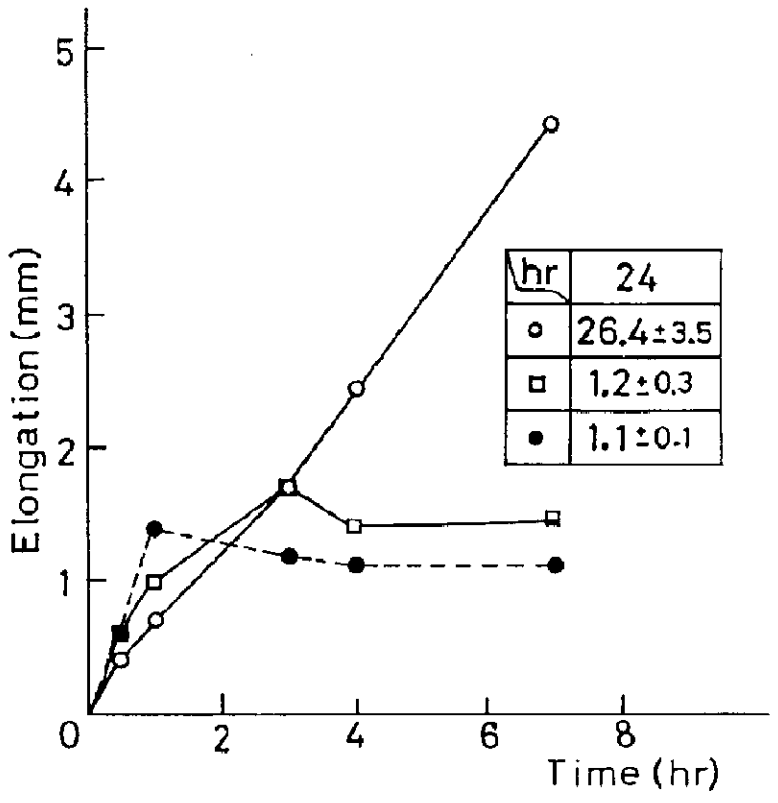

Fig. 12. Results of acidification treatments. (○———○) Control, (□———□) HCl and (●- - - - -●) acetate buffer at 25 ± 1° C using 10 roots for each. Inset: table of elongation after 24 h.

in buffer tended to elongate upward, i.e., against gravity. A photograph is shown in fig. 13b. Once the roots exceeded the surface of the medium, they grew with the usual velocity. We wanted to investigate the continuous application of entire acidification on roots, hence we inclined the vessel. In this situation the roots could no longer jut out.

Fig. 12 demonstrates that the acidified roots cannot grow over a long period of 10 h in spite of the facilitated elongation at early stages of 1 h or so. This result is surely in agreement with our expectation based on the experiment of electric isolation plus HCl treatment in fig. 6. Furthermore, it does not contradict the conventional acid growth mechanism. In these kinds of studies using the short segment of root as well, the facilitation effect of acid on growth continues for only 1–2 h at most [34–37].

5.2. Temporal changes in spatial patterns of electric potential and enzyme activity

Fig. 14 shows the temporal change in the electric spatial pattern measured with the multi-electrode system with acetate buffer treatment. We can point out from fig. 14 the following facts: The electric potential displays a typical alternating spatial pattern along the root at early stages over 1 h. At intermediate stages of a few hours, however, the pattern tends to broaden along the root accompanied by the disappearance of two peaks around 3 and 12 mm from the tip. The pattern for periods over several hours no longer shows the distinct alternating structure. These results seem to conform with those in fig. 12 that the roots with facilitated growth only for the initial 1 h are destined to decline after the passage of several hours.

The temporal changes in invertase activity are shown in fig. 15. A peak around 5 mm from the tip declines gradually to disappear in 2 h. This

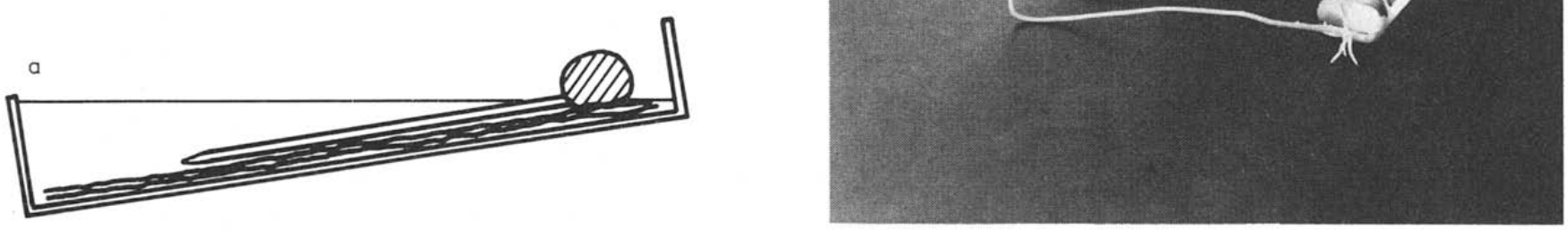

Fig. 13. Experimental situation (a) and photograph of roots (b). The upper part in (b) refers to the usual growth, and the lower concerns the abnormal growth when the root was laid horizontally in the acetate buffer.

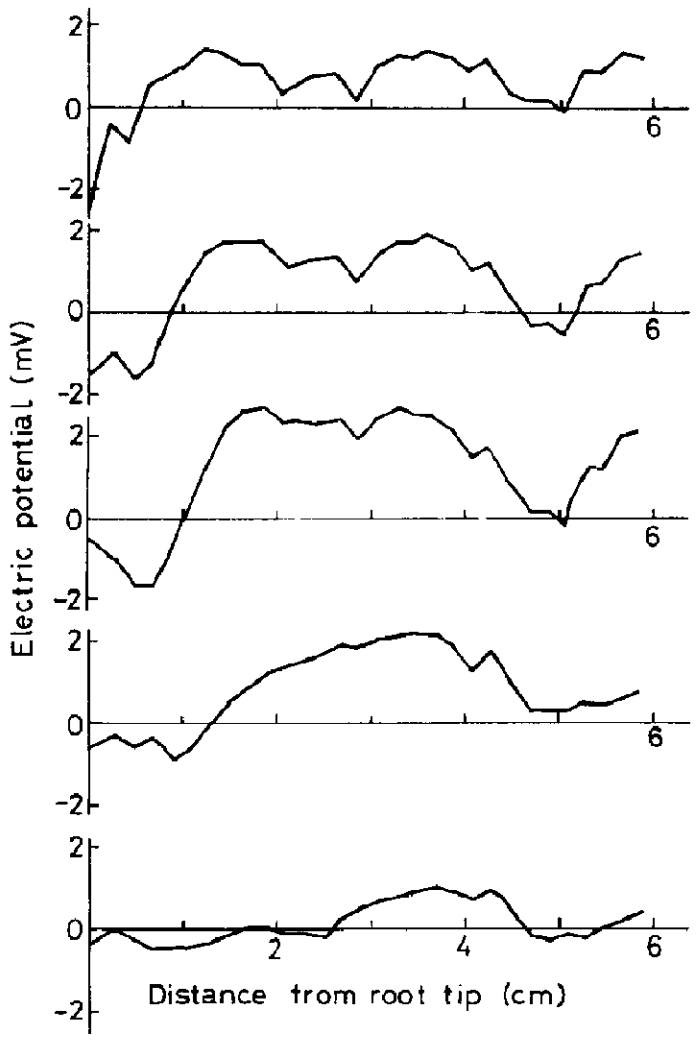

Fig. 14. Change in electric spatial pattern with time in a root of about 7.5 cm length treated with acetate buffer. The first from the upper was measured after 15 min from the onset, the second 1 h later, the third 1 h 40 min later, the fourth 2 h later and the fifth 6.5 h later.

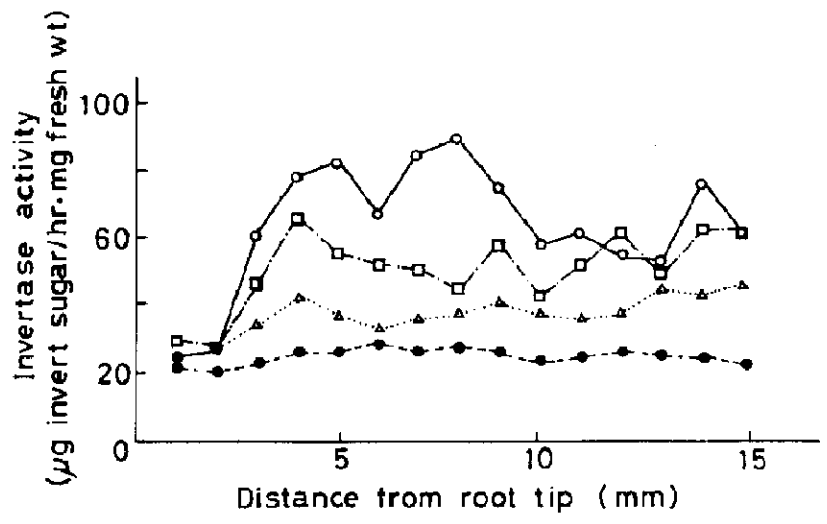

Fig. 15. Temporal change in invertase activity (average over 10 collected roots) along a root treated with acetate buffer. (○———○) Original at the start of experiment, (□·-·-·□) 30 min later, (△·····△) 1 h later and (●- - - - -●) 2 h later.

result also corresponds to the root growth in fig. 12.

From these results we can deduce an intimate relation among the growth, electric-potential profile and enzyme-activity pattern. The growth shows a parallel decline to the flattening electric-potential and enzyme-activity patterns along the root. The initial growth in fig. 6 can be considered as being brought about through acid elongation. This kind of growth may be a direct consequence of the acid growth mechanism, which is independent of energy production and consumption. It belongs to the 'passive' property that the cell wall is expanded through acidification.

Long exposure, however, to entire acidification causes destruction of the H^+ concentration gradient along the root. This gradient is maintained with such an 'active' property dependent on energy metabolism as the spontaneous emergence of electric-potential and enzyme-activity patterns along the root. In turn, the weakened H^+ concentration gradient leads to extinction of these patterns probably through some physicochemical steps, since all these factors are mostly intimately coupled with each other [5,6,38]. This may affect the transport of species necessary for growth such as auxins. As a consequence, we can explain those experimental results comprehensively by dividing the growth step into two parts, i.e., the passive part of cell wall expansion and the active part of spontaneous formation accompanied by energy metabolism represented by electric-potential and enzyme-activity patterns. The latter can be considered as a self-organized structure appearing far from equilibrium.

An experiment also suppressing the initial growth was performed by employing 30 mM phosphate buffer (pH 7.0) with the roots. The growth was retarded in any period, and the typical peak of invertase activity around 5 mm from the root tip disappeared finally (data not shown). While it might be possible that normal membrane functions are affected by this concentrated phosphate buffer, it is noticeable that the biochemical activity within the root is also changed. Since the potential drop in the 30 mM buffer solution was evident, electric measurement was not made. As expected for the present case, the initial remark-

able elongation was not induced owing to the lack of tip acidification. This confirms our conclusion in fig. 12 that the acid growth mechanism can be applicable to explanation of the initial elongation.

6. External electric disturbance

Roots can grow spontaneously by forming spatial patterns of electric potential and enzyme activity. In other words, these spatial patterns may be adequate for growth so that H^+ can be effectively transported to the elongation zone. As shown in Characean systems [5], the pattern appears according to the principle of minimum energy dissipation or minimum entropy production [8]. In bean roots, we can also expect the effectivity of this principle. If we disturb electrically the spontaneous pattern commensurate to growth, the root is anticipated to show abnormal growth. This was performed by placing roots on an electric conductor coated with carbon.

Fig. 16 demonstrates the original and disturbed patterns of electric potential near the root surface. The measurements were made by using the multi-electrode system. The original has a peak around 5 mm from the tip; but the disturbed pattern no longer shows a peak and gives rise to the unusually large electric potential along the root. The elongation of roots under electric disturbance is compared with that in distilled water in fig. 17. Ten roots were used in each experiment. Fig. 17 reveals that growth under electric disturbance is retarded. Reliable measurements during periods over 4 h could not be made because the roots under disturbance tended to curve in a complicated manner.

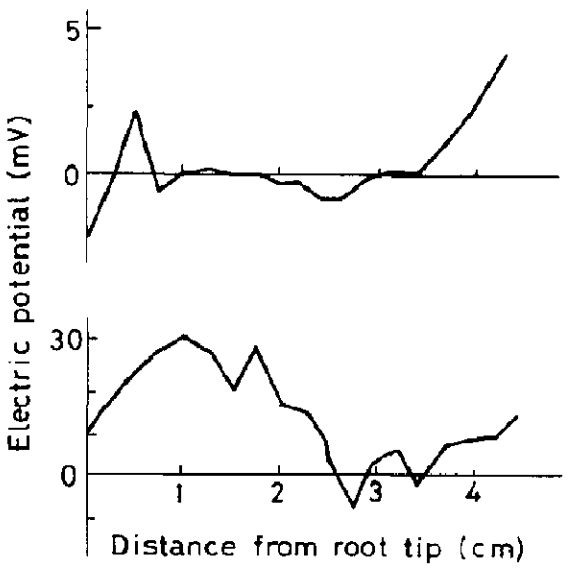

Fig. 16. Electric potential of a root of about 5 cm length under electric disturbance measured with the multi-electrode system. The upper part corresponds to the potential in a normal root under the usual conditions, and the lower concerns the result in the root under electric disturbance. Note that the peak located 5 mm behind the tip disappeared and the absolute value was extremely large, i.e., 30 mV, under electric disturbance.

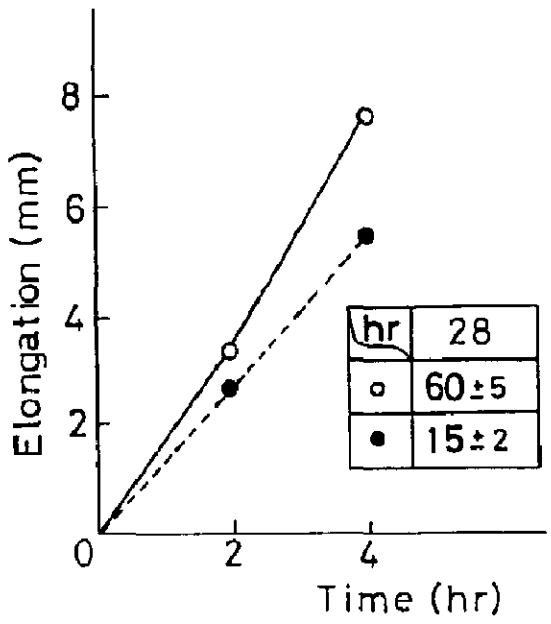

Fig. 17. Elongation of roots under electric disturbance at 30±1°C. (○———○) Control and (●·-·-·●) under disturbance. Since the root under electric disturbance curved to a large extent, a rough estimate of elongation after 28 h is shown in the inset.

These results can be interpreted as being caused by the perturbation of efficient H^+ flow around the root. It may inhibit the continuous supply of H^+ in the elongation zone to cause the wall expansion. The disturbed pattern in fig. 16 may become unfavorable from the viewpoint of minimum energy dissipation. It may be adequate for the growth. The second possibility may be an effect on various transport systems within the root, since most transported species have electric charges. The third possibility is the production of chemicals such as Cl_2 by the electric cell, which may directly affect the growth of root. At present, however, it is not easy to decide whether the growth was affected by the electric field or the chemicals produced. These factors may be considered to act together on growth.

7. Discussion

The electric spatial pattern and the enzyme activity pattern appearing in the growth process were studied here. We found that the first peak of electric potential around 5–7 mm is located close to the peak of invertase activity, a little behind the elongation zone. The electric potential along the root showed a band-type pattern with a spatial period of approx. 2 cm, tending to become more positive at the side of root base than near the root tip as a whole. The experiments on electric isolation and the tip acidification treatment revealed that H^+ is transported in the external medium resulting in the cell wall expansion. The entire acidification of a root gave the initial facilitated growth, but later retarded the growth. Both the electric potential and the enzyme activity diminished gradually with time in parallel with the decline of growth. Roots showed a rather slow growth speed on application of an electric disturbance so that the original electric pattern produced by the roots themselves might be changed greatly. This result was interpreted as being due to the perturbation of efficient H^+ flow around the root to the elongation zone and the electric effect on transported species such as auxins inside the root.

Fig. 18 illustrates the electric flow pattern suggested from the above experiments. The electric current flows into the root-tip side, accompanied by some local current loops in the mature zone of the long root of 10 cm or so. This kind of pattern in a multicellular system can be considered to appear in a similar mechanism to the banding in unicellular systems as in Characean internode [5]. A nonlinear coupling of the H^+ flux across the cell membrane with ATP concentration, enzyme activity and auxin concentration may cause the appearance of a self-organized structure far from equilibrium. In terms of nonequilibrium thermodynamics [8], this kind of structure can be called a dissipative structure. Particularly in the present case, the electric events may be intimately related to the formation of a pattern; hence we can call the banding patterns in bean roots and Characean cells an 'electric dissipative structure'. The maintenance of this structure may require an energy metabolism process working far from equilibrium, in contrast to tip elongation through acidification.

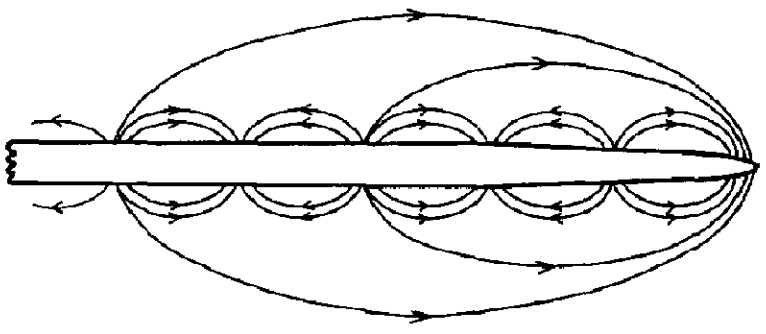

Fig. 18. Qualitative property of electric current around a root of about 10 cm length. Electric current flows into the root-tip side, accompanied by some local current loops in the mature region.

Let us next discuss the relation of the electric dissipative structure to growth. The tip elongation is facilitated by the supply of H^+ to the elongation zone, as can be seen from fig. 18. A detailed illustration of the events occurring near the root tip is given in fig. 19 according to the present experimental results. The H^+ pumps at the surface work actively in the mature zone slightly behind the elongation zone, where the surface electric potential and the invertase activity are relatively high. H^+ accumulating near the cell wall of the elongation zone causes the wall expansion as inferred from the acid growth mechanism [11,12]. In

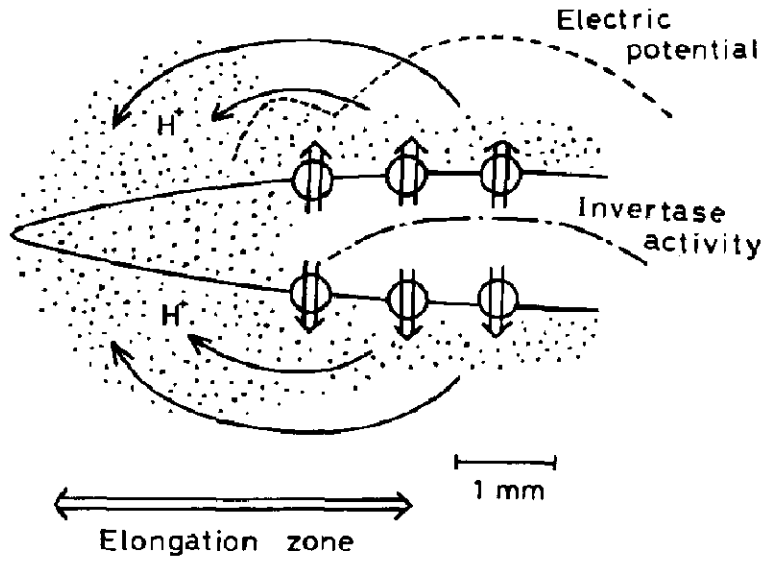

Fig. 19. A proposed model for root growth. A root near the tip immersed in aqueous medium at the stage near the resultant equilibrium state is illustrated. In this stage, H^+ accumulates near both the root tip and the immature elongation zone at 1–3 mm. H^+ is pumped from the semi-matured elongation zone at 3–5 mm and mature region, to be transported in the external medium.

turn, the newly produced mature zone can transport H^+ into the root tip. The electric dissipative structure is formed spontaneously along the whole root, associated with energy metabolism, to cause electric flow into the elongation zone.

Conflicting evidence concerning tip acidification deserves comment. Weisenseel et al. [27] reported a relative alkalinization of pH 5.5–6.0 in the elongation zone (external medium pH 5.0). Whereas a similar result was obtained by O'Neill and Scott [37], these results apparently disagree with many reports supporting tip acidification [11,39,40] as well as the present result in table 1. To resolve this conflict, we must note that the cell wall has only to receive H^+ necessary for loosening; the aqueous solution near the cell surface need not always be acidified. In fact, the pH will not be lowered if all H^+ is consumed to loosen the wall even when H^+ is supplied from the mature zone. In this case, acidification could not occur but alkalinization might be observed. In addition, the measuring time must be taken into account, because the H^+ concentration pattern changes with time as shown in fig. 8. Since the electric spatial pattern is rather dynamic as long as the root is short (see details in the appendix), the pH pattern can also be altered in this situation. We can therefore expect both the tip acidification and relative alkalinization according to the experimental conditions. In both cases, however, the acid growth mechanism is effective, only concerned with the tip elongation. H^+ can be transported from the mature zone to the elongation zone through patterned activation of H^+ pumps emerging as the electric dissipative structure. In other words, the acid growth mechanism can only be applicable to the description of a local property such as tip elongation. In contrast, the new mechanism proposed here concerning the electric dissipative structure is adequate for a global description of growth including the spatio-temporal organization along the entire root.

It has been recently found that anoxia diminishes the electric pattern along a root (data not shown). In this case, the disappearance of the pattern occurred rapidly within a few minutes at the tip region, and later extended to the mature region. After several tens of minutes, a nearly homogeneous pattern was realized. While detailed analysis is in progress the above result means that a typical electric pattern such as that in figs. 4 and 5 is formed through energy metabolism in a similar manner to Characean banding. This inference supports the above suggestion of dissipative structure.

As detailed in the appendix, the small peak or flat part of the electric potential around 2–3 mm behind the root tip can sometimes appear (figs. 5, 14 and 22). This region corresponds to a somewhat rearward part of the elongation zone, i.e., the semi-matured elongation zone. This observation may imply that H^+ is extruded from the surface in this region. In this case, therefore, we can expect that one part of the elongation zone adjoining the mature region can also supply H^+ to the other part of the elongation zone near the root tip, which is quite immature, in a cooperative fashion with the mature region. Fig. 19 is illustrated so as to contain this case widely. In relation to that fact, it should be noted that the electric current is composed of several ion species such as H^+, K^+ and Na^+. Thus, a direct conclusion of H^+ flow may require further electrochemical study. According to the flow patterns of other ion species, the H^+ flow pattern may be altered. As shown in the appendix, such an electric pattern can be considered as rather dynamic.

The present experiments deal mainly with the electric potential in the external medium and the invertase activity, ATP and H^+-ATPase within the root. For further investigation of the detailed biophysical characteristics of an electric dissipative structure, electric measurement within a root may also be required. Two kinds of transport systems were found at the plasma membrane and the surface of xylem in roots and stems [41–43]. This may imply the existence of H^+ flow within the root as well as the stem. In this sense, we must study the relation between the external and internal electric currents. An equivalent electric circuit may be effective for this purpose. The construction of an electric circuit model of a system comprising the root and surrounding external medium enables us to elucidate the distinct flow pattern of H^+; this leads to a further understanding of growth and electricity.

From the viewpoint of the electric dissipative structure, let us now comment on the self-sustained oscillations of electric potential frequently observed in root growth [13–15]. An example of oscillation is given in fig. 24. The self-sustained oscillation is a typical phenomenon appearing far from equilibrium. A similar kind of oscillation was found in the membrane-formative process of a *Nitella* protoplasmic droplet [44]. A recent study based on nonequilibrium thermodynamics [45] showed that the oscillation arises with the membrane formation and destruction occurring in local areas on the surface of the droplet. To take account of this result may suggest the participant role of the membrane-formative process in the elongation zone in roots as well. In fact, these oscillations emerging in real biological systems can also be reproduced well in artificial membrane systems composed of lipids [45–52]. These kinds of oscillations are seriously affected by the pressure applied to the membrane. The self-oscillations in roots may also be directly related to the turgor pressure [13,14]. Growth can thus be considered as a typical nonequilibrium phenomenon exhibiting a spatio-temporal organization through the membrane.

In a thermodynamic sense, the spatial patterns of electric potential, enzyme activity and ATP studied here are analogous to the spatial aggregation pattern of a slime mold [8]. In this system, the cyclic AMP distribution plays an important role in morphogenesis; a theoretical analysis of the reaction-diffusion type was made in detail for this kind of chemical dissipative structure [53]. A theoretical analysis of the electric dissipative structure in roots is a future task. Ca^{2+} accumulation near the root apex was reported [54]; the effect of this factor on growth may be very important as has often been suggested [6,38,44,45,55]. The inhomogeneous distribution of Ca^{2+} may have an intimate relation with the spatial patterns of electric current and enzyme activity. The role of plant hormones of auxins in the formation of an electric spatial pattern along a root was not pursued in the present study. A biochemical study correlating the role of hormones with the electric events is necessary. Nevertheless, electrical nonequilibrium theories treating the dynamic interaction between biological systems and the environment may provide a revealing way of analyzing the growth and electricity. Along this line, it may become possible to control the growth speed by some adequate electric treatment in the near future.

Appendix

Here the stability of an electric banding pattern and the dynamic characteristics of an elongation zone are described in detail. Fig. 20 shows the formation of bands as the root elongates. While the root length is as short as 2 cm, a convex peak exists around 5 mm behind the root tip. The root growing to about 5 cm usually has two or three peaks in the elongation and mature regions. When the root grows to 10 cm or so, a clear banding pattern can appear. The period is approx. 2 cm. These electric bands are rather stable over a few hours (ref. 10 and see fig. 22). However, the electric pattern is occasionally unstable when the root is short. Fig. 21 demonstrates this fact, using a root of about 4 cm length. One set of measurement of curve (i) was made 1 h after the other (ii).

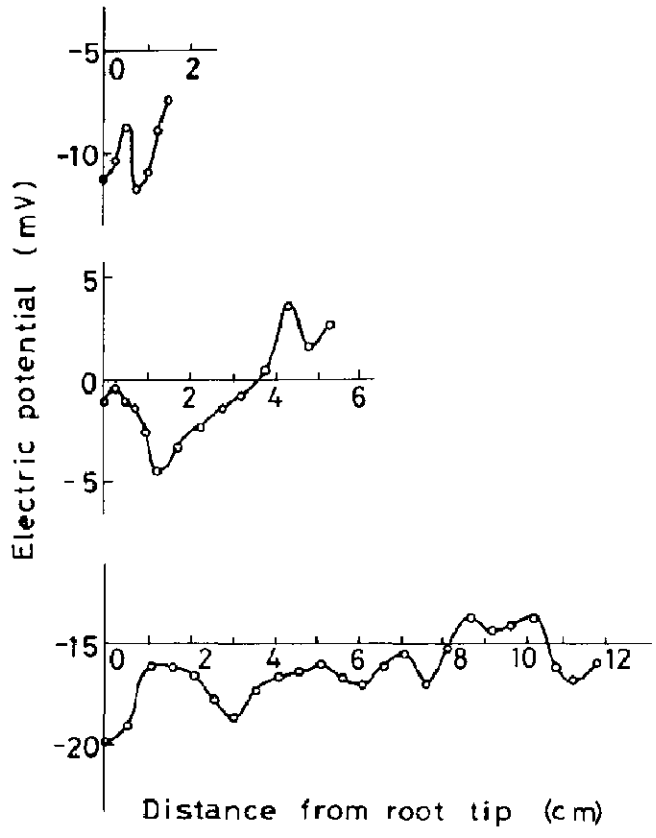

Fig. 20. Change in electric pattern with growth. The middle panel was obtained from measurement made 26 h after the top, and the bottom to that 38 h later than the middle panel.

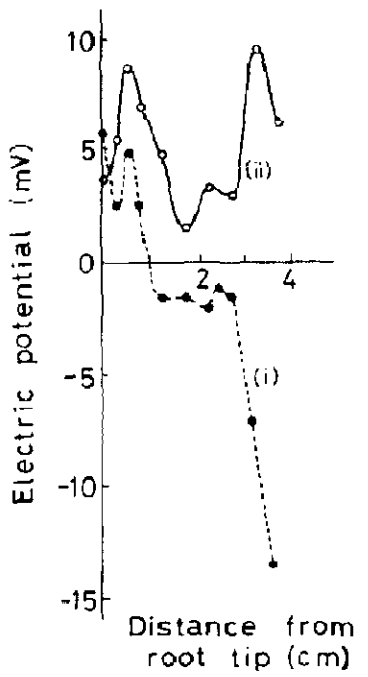

Fig. 21. Surface electric potentials for a short root of about 4 cm length. Curve (i) is obtained 1 h later than curve (ii).

Curve (i) shows that the electric potential around 2 mm is higher than around 1 cm behind the tip. On the other hand, in many cases using long roots, the root was electrically more positive around 1 cm than around the tip, as shown in figs. 4, 5, 20 and 22. For the short length of the root, the reversed pattern shown by curve (i) can be sometimes found. This kind of observation concerning the negative potential near 1 cm behind the tip in the short root has been reported by Lund and coworkers [9,56] using an onion root of length 3–4 cm. Furthermore, a similar tendency for the electric pattern being relatively mobile for a short individual has also been found in Characean internodes [57].

The electric bands formed in the mature zone of long roots are stable, but the electric pattern in the elongation zone is very dynamic. Fig. 22 shows an example obtained using the multi-electrode system. As can also be seen from fig. 23, the pattern with about 2 cm period exists stably as a whole. Near the root tip, however, a new small peak was added to the existing peaks with elongation of the root (about 2 mm for 100 min). During this process, a self-sustained electric oscillation appeared with a temporal period of about 6 min (fig. 24). The elongation zone lay at the positions of electrodes 1, 2 and 3 at the start of experiment; it later deviated to positions 2, 3 and 4. Position 4, located first at the root tip, not oscillating during the initial stages, became oscillatory. The phase of the oscillation at position 4 (1.3 mm behind the tip, finally) was different from point 2 (3.9 mm behind the tip, finally), which changed to belong to the

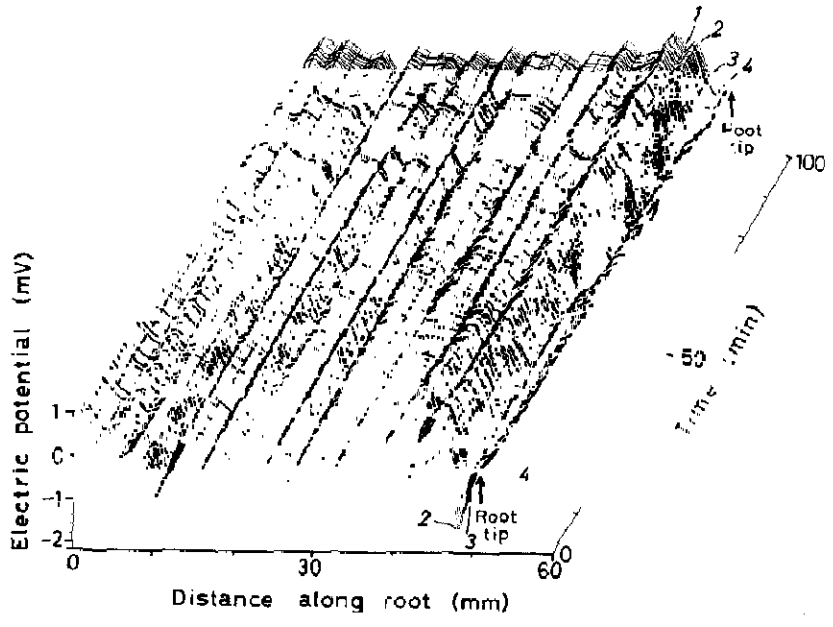

Fig. 22. Spatio-temporal pattern of electric potential with growth. At the start of the experiment, the root tip was near electrode 4. The root elongated about 2 mm when measurement was completed. Position 2 located first in the elongation zone changed almost to the mature region 100 min later. A new small peak was added to the elongation zone, associated with the electric oscillation, which started at about 50 min. The temporal variations at fixed points are shown in fig. 24.

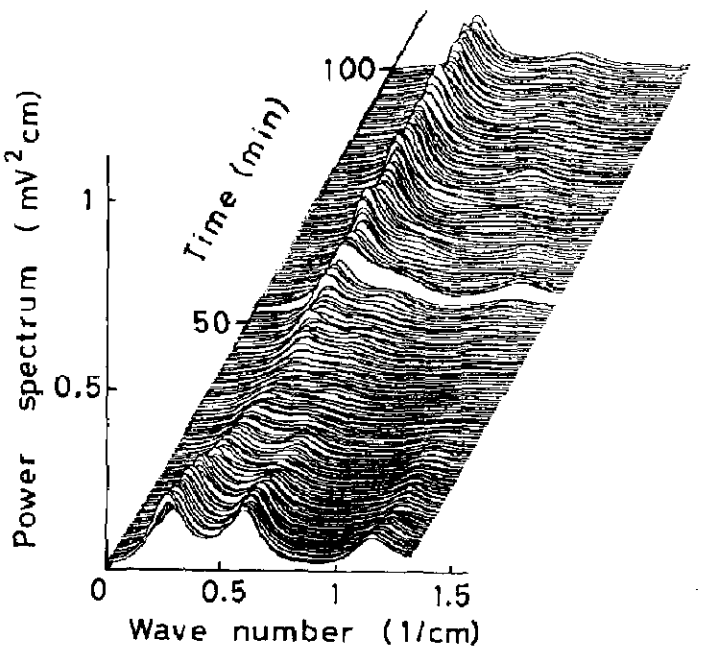

Fig. 23. Power spectrum showing the stability of the electric banding pattern. The data are from fig. 22. Fourier analysis of electric spatial pattern was made by the use of MEM (maximum entropy method).

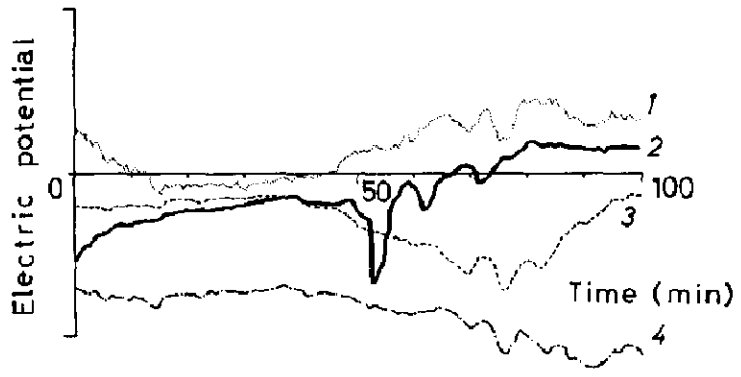

Fig. 24. Appearance of electric oscillation during the formative process of a new peak in the elongation zone. Numbers 1–4 correspond to the electrode numbers in fig. 22. To facilitate comparison of oscillations, the full scale and origin are modified: full scale of axis of the ordinate is 2 mV for curves 1 and 4, 6 mV for curve 2, and 4 mV for curve 3. Curve 4 is shifted to a lower position, −0.5 mV. Note that the electric potential of curve 2 became positive, accompanied by a large-amplitude oscillation.

mature region or the rear part of the elongation zone after several tens of minutes. These observations imply that the electric potential near the elongation zone is rather dynamic compared with the mature region: the small peak is added gradually associated with self-oscillations, while the overall spatial period is almost maintained along the root to approx. 2 cm, as understood from fig. 23. The detailed measurement for pursuing a process in which such a long period of 2 cm is formed stably with elongation is the subject of a future work.

A small peak or a flat part near the tip can often be observed, as shown in fig. 5. In this case, we can consider that H^+ is extruded in this elongation region. This might be related to the experimental result on the electric current flowing around a vertically oriented *Lepidium* root, using a vibrating probe along the root surface [58]. According to this result, the electric current flows out of the rear part of the elongation zone and then flows into the front part of the elongation zone and the meristem zone. In this experiment, however, we must note that the root used is very short, e.g. 6 mm, in order to investigate the mechanism of geotropism inherent to the relation between meristematic and elongation zones. Therefore, a direct comparison with the result in fig. 22 for a very long root may not be easy, because the elongation region occupies most of the root length for the case of short roots, and the electric pattern changes as the root elongates (fig. 20). Furthermore, it should be noted that for a long root the electric current is not determined from the local pattern but from the whole pattern of electric potential through the superposition along the root, containing the elongation and mature regions.

Acknowledgement

The authors would like to express their sincere thanks to Miss Y. Matsuki for technical assistance in measurements of ATP content and H^+-ATPase activity.

References

1 R. Nuccitelli and L.F. Laffe, J. Cell Biol. 64 (1975) 636.
2 D.G. Spear, J.K. Barr and C.E. Barr, J. Gen. Physiol. 54 (1969) 397.
3 J.-P. Metraux, P.A. Richmond and L. Taiz, Plant. Physiol. 65 (1980) 204.
4 N.A. Walker and F.A. Smith, J. Exp. Bot. 28 (1977) 1190.
5 K. Toko, H. Chosa and K. Yamafuji, J. Theor. Biol. 114 (1985) 127.
6 K. Toko, S. Iiyama and K. Yamafuji, J. Phys. Soc. Jap. 53 (1984) 4070.
7 K. Toko and K. Yamafuji, J. Phys. Soc. Jap. 51 (1982) 3049.
8 P. Gransdorff and I. Prigogine, Thermodynamic theory of structure, stability and fluctuations (Wiley-Interscience, Gordon, 1971).
9 E.J. Lund, Bioelectric fields and growth (University of Texas Press, Austin, 1947).
10 S. Iiyama, K. Toko and K. Yamafuji, Biophys. Chem. 21 (1985) 285.
11 T.J. Mulkey, K.M. Kuzumanoff and M.L. Evans, Planta 152 (1981) 239.
12 D.L. Rayle and R.E. Cleland, Plant Physiol. 46 (1970) 250.
13 I.S. Jenkinson, Aust. J. Biol. Sci. 15 (1962) 101.
14 B.I.H. Scott, Ann. N.Y. Acad. Sci. 98 (1962) 890.
15 K. Toko and K. Yamafuji, The theory of dynamical systems and its applications to nonlinear problems, ed. H. Kawakami (World Sci., Singapore, 1984) p. 228.
16 K. Hayashi, K. Toko and K. Yamafuji, Tech. Rep. Kyushu Univ. 58 (1985) 263 (in Japanese).
17 H. Miyake, T. Ikehara, T. Sakai and H. Yamaguchi, Acta Med. Kinki Univ. 1 (1976) 75.
18 W.D. McElroy, H.H. Selinger and E.H. White, Photochem. Photobiol. 10 (1960) 153.

19 Y. Kagawa, Methods in membrane biology, ed. E.D. Korn (Plenum Press, New York, 1974) p. 201.
20 J.M. Nelson, J. Biol. Chem. 153 (1944) 375.
21 M. Somogyi, J. Biol. Chem. 195 (1952) 19.
22 B. Novak, Adv. Chem. Phys. 29 (1975) 281.
23 K. Esau, Plant anatomy (John Wiley, New York, 1941) p. 470.
24 K.L. Edwards and T.K. Scott, Planta 119 (1974) 27.
25 H. Kitasato, J. Gen. Physiol. 59 (1968) 60.
26 U. Kishimoto, N. Kami-ike, Y. Takeuchi and T. Ohkawa, J. Membrane Biol. 80 (1984) 175.
27 M.H. Weisenseel, A. Dorn and L.F. Laffe, Plant Physiol. 64 (1978) 512.
28 W.J. Lucas and R. Nuccitelli, Planta 150 (1980) 120.
29 A.L. Hodgkin and A.F. Huxley, J. Physiol. 117 (1952) 500.
30 J.A. Hellebust and D.F. Forward, Can. J. Bot. 40 (1962) 113.
31 R. Sexton and J.F. Sutcliffe, Ann. Bot. 33 (1969) 407.
32 R.A. Jones and P.B. Kaufman, Plant Physiol. 55 (1975) 114.
33 R.L. Lyne and T. ap Rees, Phytochemistry 10 (1971) 2593.
34 M.J. Vesper and M.L. Evans, Proc. Natl. Acad. Sci. U.S.A. 76 (1979) 6366.
35 B. Brummer, H. Felle and R.W. Parish, FEBS Lett. 174 (1984) 223.
36 A. Hager, H. Menzel and A. Krauss, Planta 100 (1971) 47.
37 R.A. O'Neill and T.K. Scott, Plant Physiol. 73 (1983) 199.
38 L.F. Jaffe, Membrane transduction mechanism, eds. R.A. Cone and J.E. Dowling (Raven Press, New York, 1979) p. 199.
39 T.J. Mulkey and M.L. Evans, Science 212 (1981) 70.
40 J.-M. Versel and G. Mayer, Planta 164 (1985) 96.
41 D.J.F. Bowling, Planta 108 (1972) 147.
42 H. Okamoto, K. Ichino and K. Katou, Plant Cell Environ. 1 (1978) 279.
43 H. Okamoto, K. Katou and K. Ichino, Plant Cell Physiol. 20 (1979) 103.
44 Y. Kobatake, I. Inoue and T. Ueda, Adv. Biophys. 7 (1975) 43.
45 K. Toko, M. Nosaka, M. Tsukiji and K. Yamafuji, Biophys. Chem. 21 (1985) 295.
46 N. Kamo, T. Yoshikawa, M. Yoshida and T. Sugita, J. Membrane Biol. 12 (1973) 193.
47 Y. Kobatake, Adv. Chem. Phys. 29 (1975) 319.
48 K. Toko, M. Tsukiji, S. Ezaki and K. Yamafuji, Biophys. Chem. 20 (1984) 39.
49 K. Toko, K. Yoshikawa, M. Tsukiji, M. Nosaka and K. Yamafuji, Biophys. Chem. 22 (1985) 151.
50 K. Yamafuji and K. Toko, Mem. Fac. Eng. Kyushu Univ. 45 (1985) 179.
51 K. Toko, M. Tuskiji, S. Iiyama and K. Yamafuji, Biophys. Chem. 23 (1986) 201.
52 A.M. Monnier, J. Membrane Sci. 2 (1977) 67.
53 M.H. Cohen and A. Robertson, J. Theor. Biol. 31 (1971) 101.
54 H.-D. Reiss and W. Herth, Planta 146 (1979) 615.
55 K. Toko and K. Yamafuji, J. Theor. Biol. 99 (1982) 461.
56 E.J. Lund, J.N. Pratley and H.F. Rosene, Publ. Inst. Marine Sci. 10 (1965) 221.
57 K. Toko, T. Fujiyoshi, K. Ogata, H. Chosa and K. Yamafuji, Biophys. Chem. (1987) in the press.
58 H.M. Behrens, M.H. Weisenseel and A. Sievers, Plant Physiol. 70 (1982) 1079.